MIXED MODE FRACTURE OF PLASMA SPRAYED THERMAL BARRIER COATINGS: EFFECTS OF ANISOTROPY AND HETEROGENEITY

Dongming Zhu[1], Sung R. Choi[2] and Louis L. Ghosn[1]

1. NASA Glenn Research Center, Cleveland, OH 44135
2. Naval Air Systems Command, Patuxent River, MD 20670

Abstract
The combined mode I-mode II fracture behavior of anisotropic ZrO_2-8wt%Y_2O_3 thermal barrier coatings was determined in asymmetric flexure loading at both ambient and elevated temperatures. A fracture envelope of KI versus KII was determined for the coating material at ambient and elevated temperatures. Propagation angles of fracture as a function of KI/KII were also determined. The mixed-mode fracture behavior of the microsplat coating material was modeled using Finite Element approach to account for anisotropy and micro cracked structures, and predicted in terms of fracture envelope and propagation angle using mixed-mode fracture theories.

Mixed Mode Fracture of Plasma Sprayed Thermal Barrier Coatings: Effects of Anisotropy and Heterogeneity

Dongming Zhu [1], Sung R. Choi [2] and Louis L. Ghosn [1]

[1] NASA Glenn Research Center, Cleveland, OH 44135
[2] Naval Air Systems Command, Patuxent River, MD 20670

This work was supported by NASA Fundamental Aeronautics Program.

Materials Science & Technology 2008
Pittsburgh, PA, USA
October 5 – 9, 2008

Abstract

The combined mode I-mode II fracture behavior of anisotropic ZrO_2-8wt%Y_2O_3 thermal barrier coatings was determined in asymmetric flexure loading at both ambient and elevated temperatures. A fracture envelope of K_I versus K_{II} was determined for the coating material at ambient and elevated temperatures. Propagation angles of fracture as a function of KI/KII were also determined. The mixed-mode fracture behavior of the microsplat coating material was modeled using Finite Element approach to account for anisotropy and micro cracked structures, and predicted in terms of fracture envelope and propagation angle using mixed-mode fracture theories.

Typical Thermal Barrier Coatings Consist of ZrO_2-(7-8)wt%Y_2O_3 Top Coat and Metallic Bond Coat

ZrO_2-8wt%Y_2O_3 is suitable because of its unique properties

- **Low intrinsic thermal conductivity**
- **Good thermal expansion match with metal substrates**
- **High temperature phase stability and excellent mechanical properties**
- **This work focuses on plasmas-sprayed coating systems**

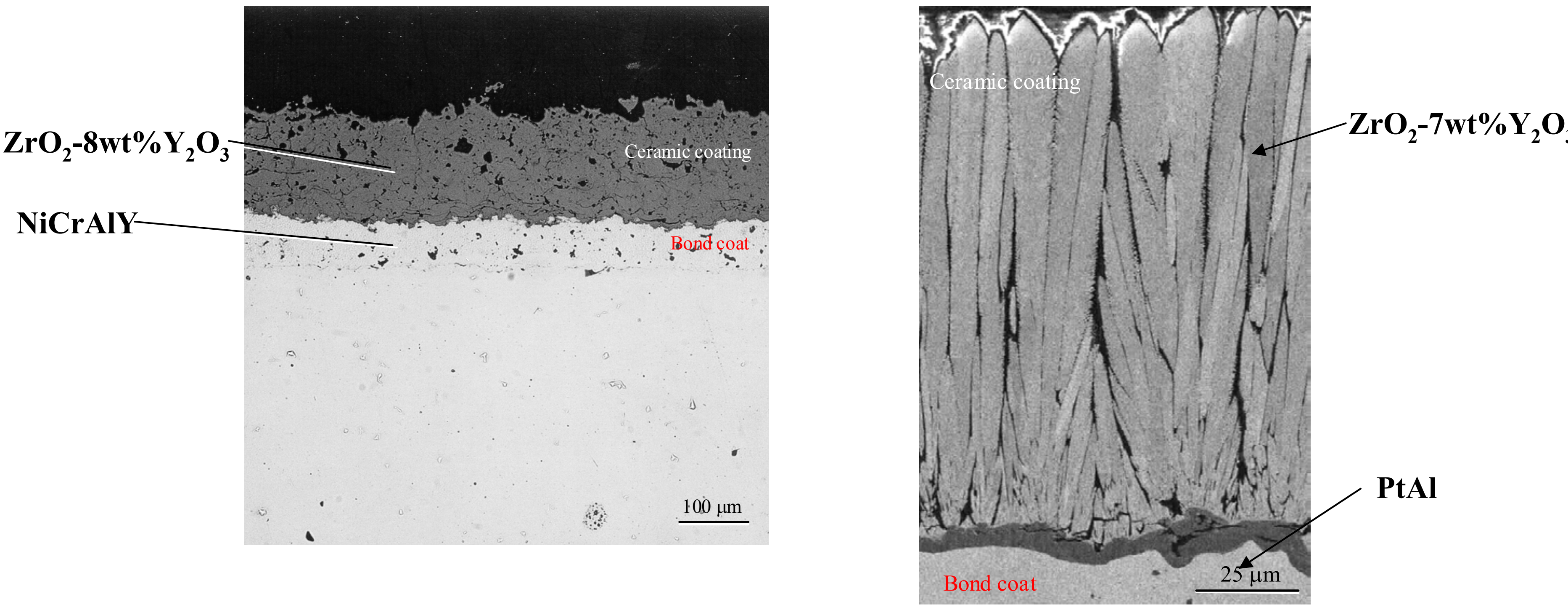

(a) Plasma-Sprayed TBC coating (b) EB-PVD TBC coating

Generalized Thermal Barrier Coating Failure Modes

— **Crack propagation is a critical issue especially under surface heat flux, thermal gradient cyclic loading**

— **Coating delamination is often resulting from mode I and Mode II mixed loading**

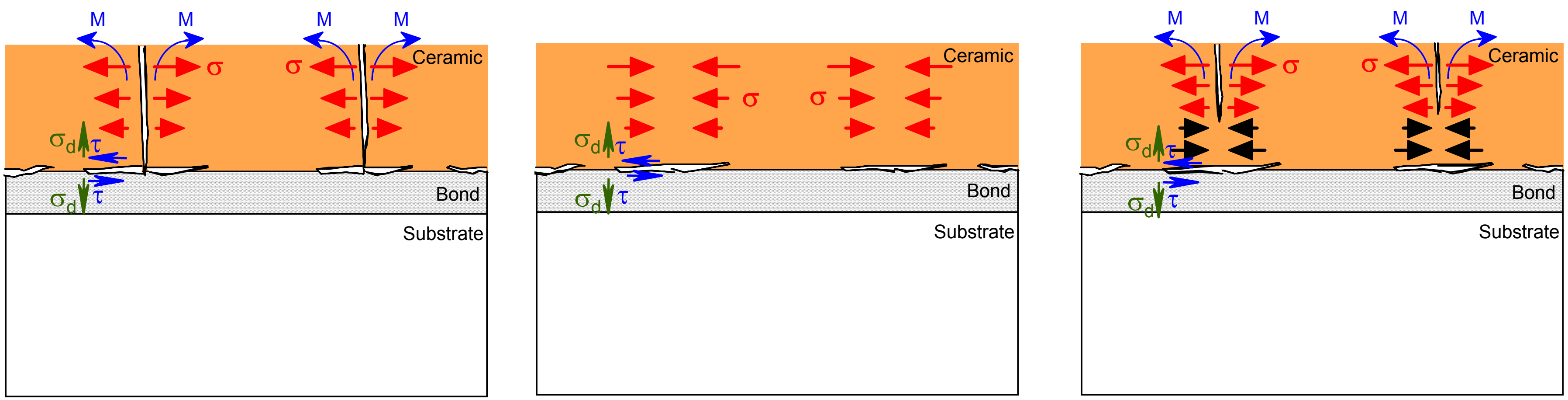

(a) High Heat Flux and Low Interface Temperature

(b) Low Heat Flux and High Interface Temperature

(c) Medium Heat Flux and Interface Temperature

Crack Propagation of ZrO_2-8wt%Y_2O_3 System under Thermal Gradient Cyclic Loading

— **Single crack growth: 0.2 mm thick TBC specimen with a 2 mm substrate center hole pre-cracked coating specimen)**

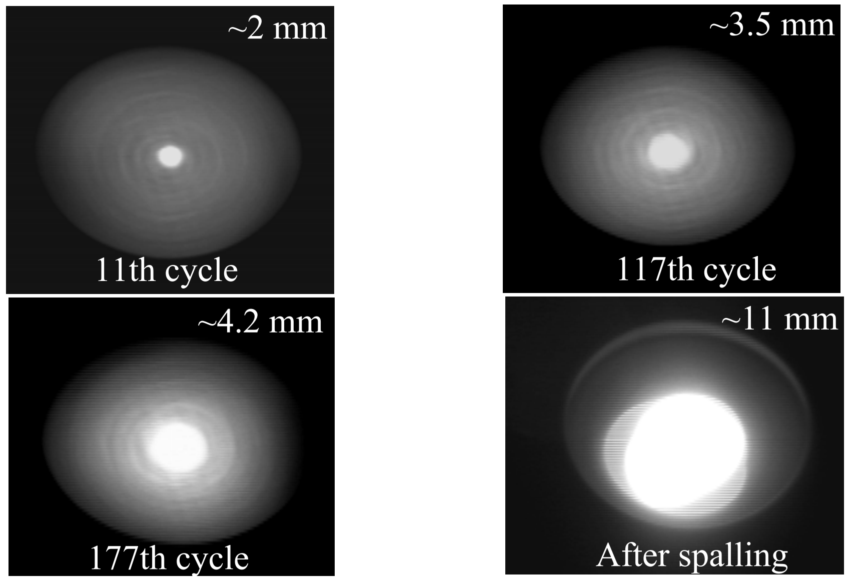

— **Typical coating delamination: non pre-cracked coating specimen under thermal gradient cyclic loading)**

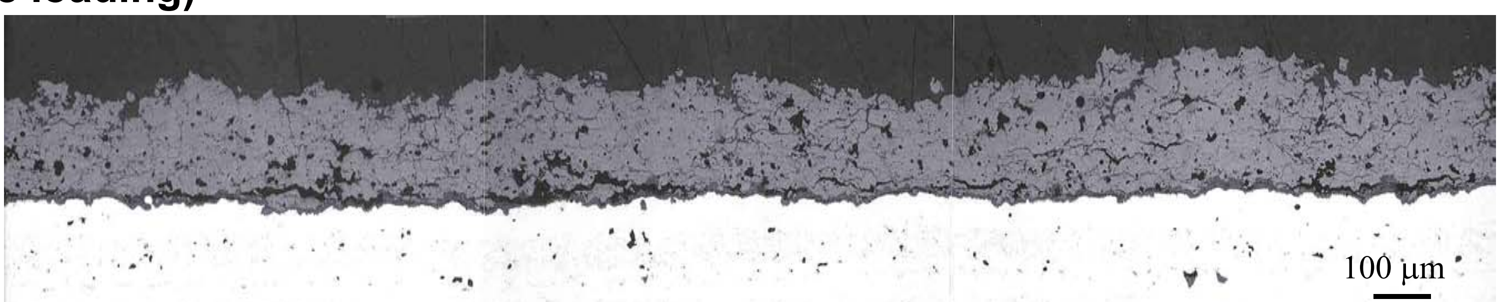

Objective

- **Determine mixed-mode (modes I and II) fracture behavior of free-standing thermal barrier coatings at both *ambient* and *elevated* temperatures**

- **Explore appropriate *mixed-mode fracture criteria* in conjunction with experimental data**

- **Finite Element Method Modeling taking into account of anisotropy and heterogeneity effect**

Asymmetric Four-Point Flexure Testing

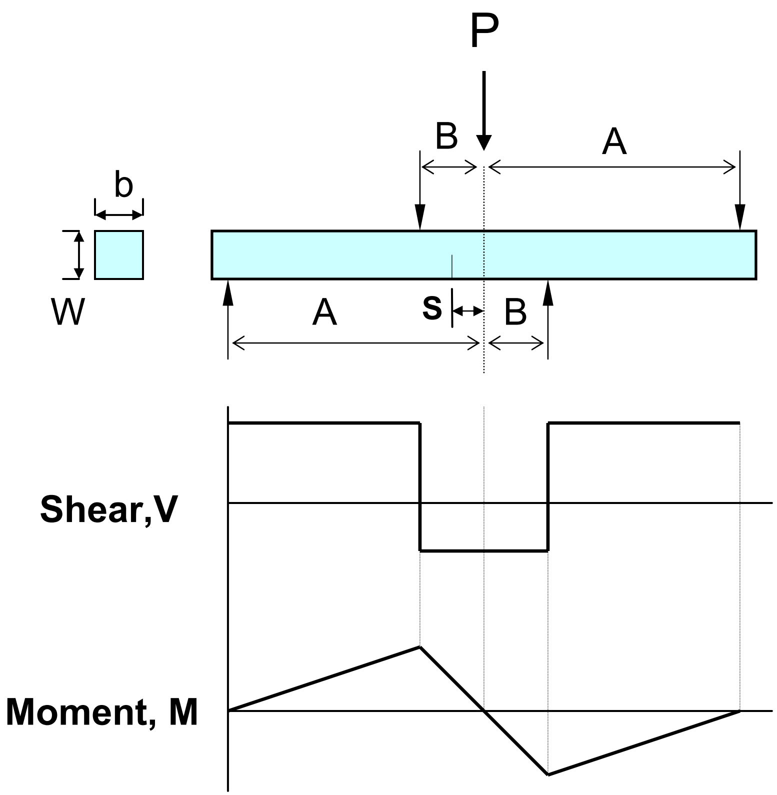

s: distance between a crack and applied load point

Shear, Moment & Stresses at 'B-B' region:

$$\text{Shear}: \quad V = \frac{A-B}{A+B} P$$

$$\text{Moment}: \quad M = Vs = \frac{A-B}{A+B} Ps$$

$$\text{Shear Stress}: \quad \tau = \frac{A-B}{A+B} \frac{P}{bW}$$

$$\text{Tensile stress}: \quad \sigma = \frac{A-B}{A+B} \frac{6sP}{bW^2}$$

The **mixity** of stresses can be changed by changing the distance 's':
* e.g. When s=0 → only shear exists (mode II); other wise, mixed modes I & II.

Experimental Procedure

Material:

- Plasma sprayed ZrO_2-8wt %Y_2O_3 thermal barrier coating
- Free standing TBC billets fabricated
- Flexure specimens [3mm(=B)x4(=W)mmx25mm] machined from billets

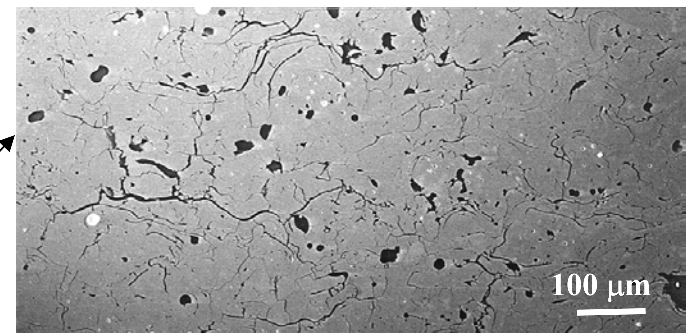

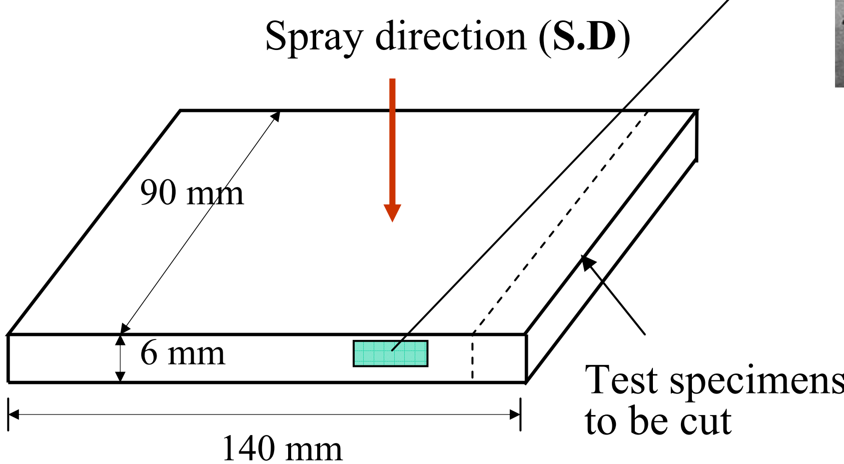

Billet

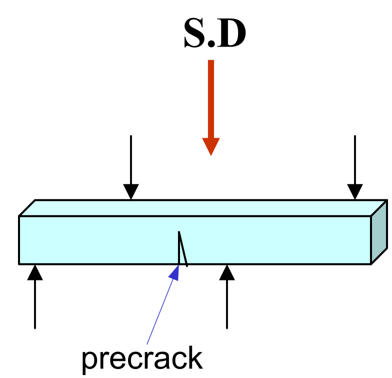

Test Specimen

Experimental Procedure

- **Sharp precracks generated**
  Single edge V-notched beam (SEVNB) method:
  Saw-notched → a sharp V-notch generated with a razor blade with 5μm diamond paste
  Precrack sizes used : $a/W \approx 0.5$
- **Test fixture configurations**
  Spans A/B = 12/6, 10/5 (typical), and 5/2.5 mm; s=0-3.6 mm
- **Test temperatures & test rate**
  25 and 1316°C in air; 0.5 mm/min in Instron 8562

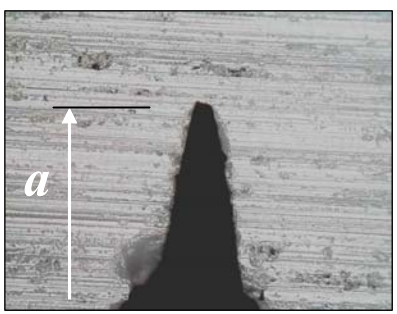

A SEVNB precrack generated
(root radius≈10-20μm)

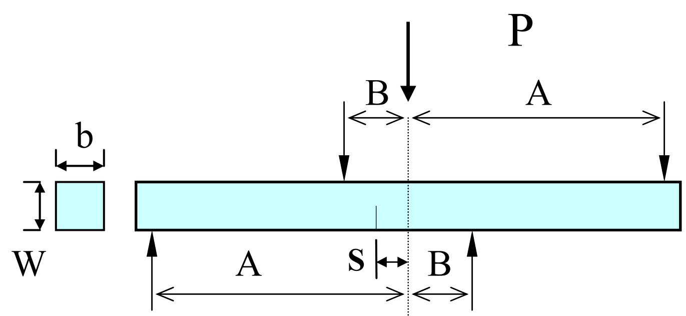

Test fixture configurations
(W=4 mm, b=3 mm)

Experimental Results

- **Mode I, Mode II, and Mixed Mode (at 25 and 1316°C)**

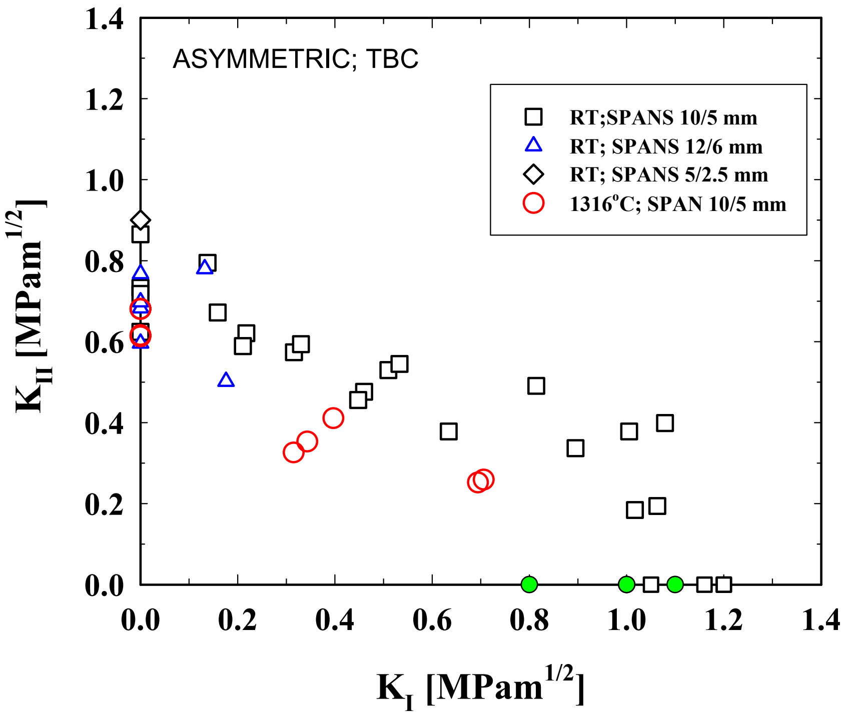

Test Temp(°C)	No. of specimens used	K_{IC} (MPa√m)	K_{IIC} (MPa√m)
25	4 in K_{IC} 9 in K_{IIC}	1.15(0.07)	0.73(0.10)
1316	4 each	0.98(0.13)	0.65(0.04)

RESULTS→

- **K_{IC} > K_{IIC}** → K_{IIC}/K_{IC}=0.64 & 0.66 (at 25 & 1316°C)
- K_{IC} and K_{IIC} at 25°C > K_{IC} and K_{IIC} at 1316°C
- **Elliptical relation** between K_I and K_{II}
- Test spans **independent**

Comparison between TBC & Dense Ceramics

– **Discrepancy observed for TBCs using energy release and strain energy based criteria**

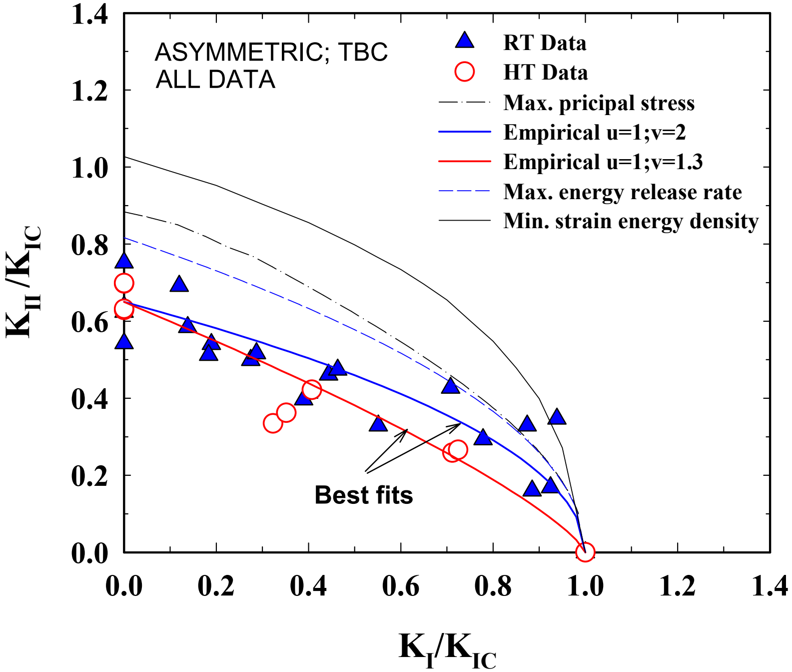

TBC (this study)

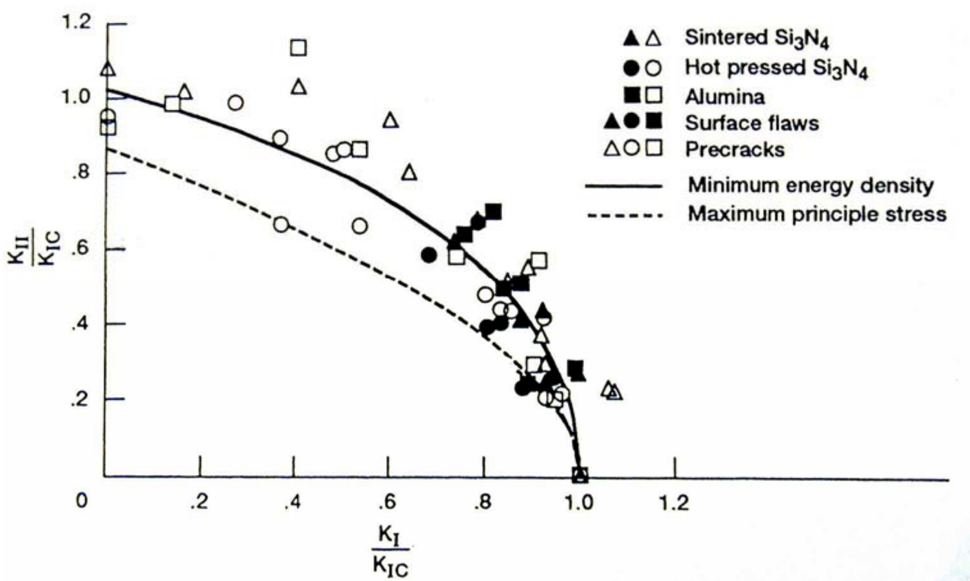

Dense Ceramics (previous study, '93)

Best fit → **'empirical'** criterion $K_{IIC} \approx 0.65 K_{IC}$

Best-fit → **'minimum strain energy density'** criterion; $K_{IIC} \approx K_{IC}$

Comparison Between TBC & Dense Ceramics

– **FEM modeling showed good agreement using anisotropic elastic modulus property data**

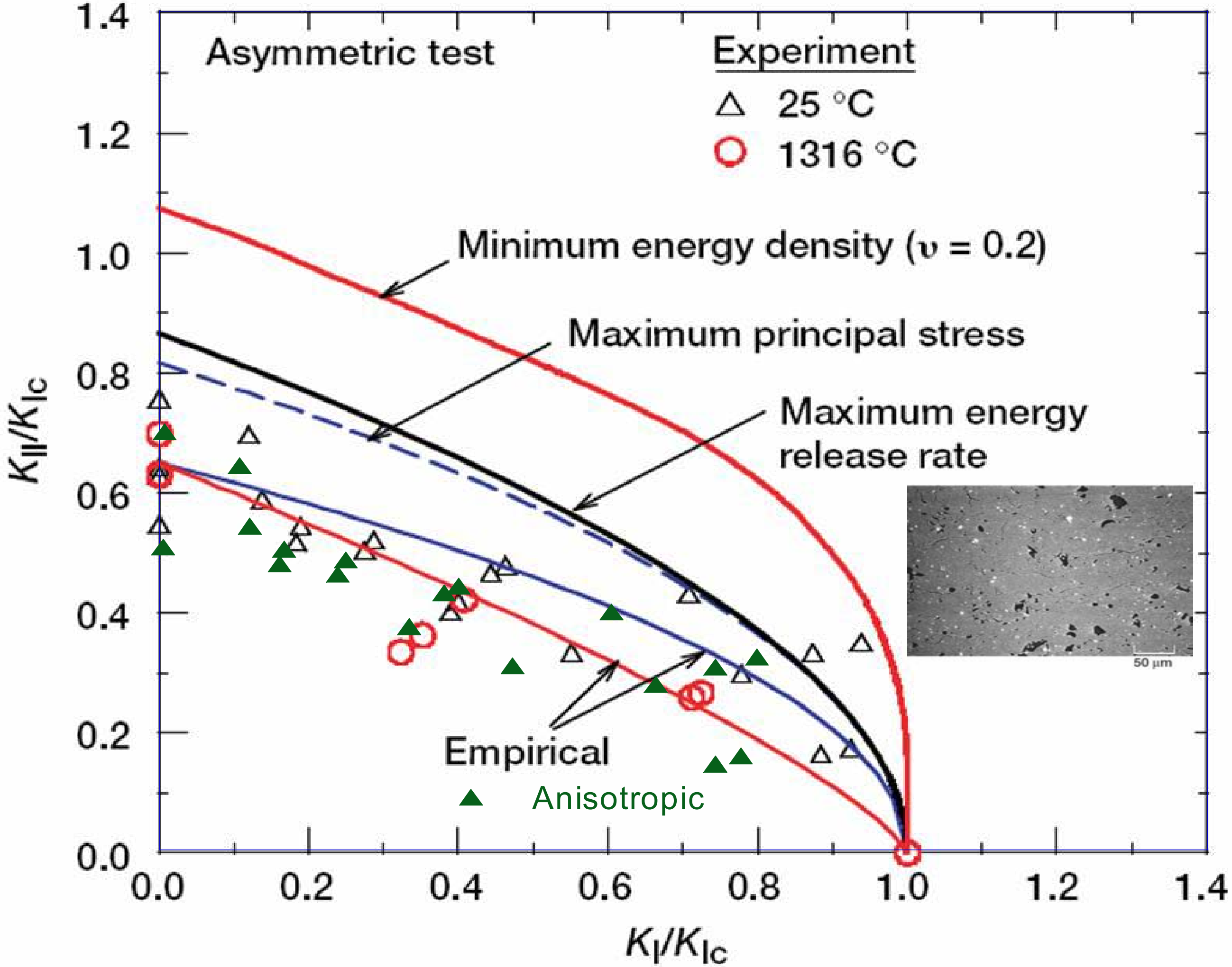

Prediction of Crack Propagation Angle with FEM Anisotropy Models

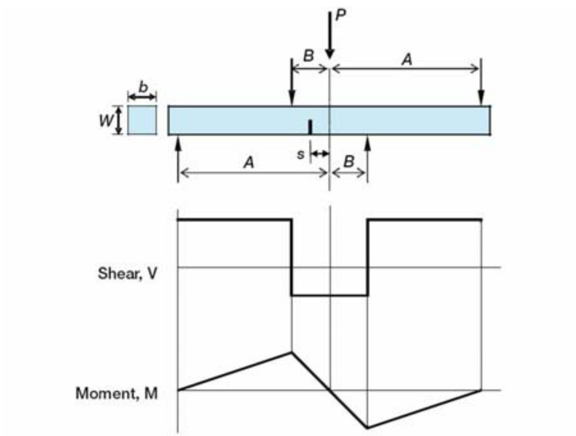

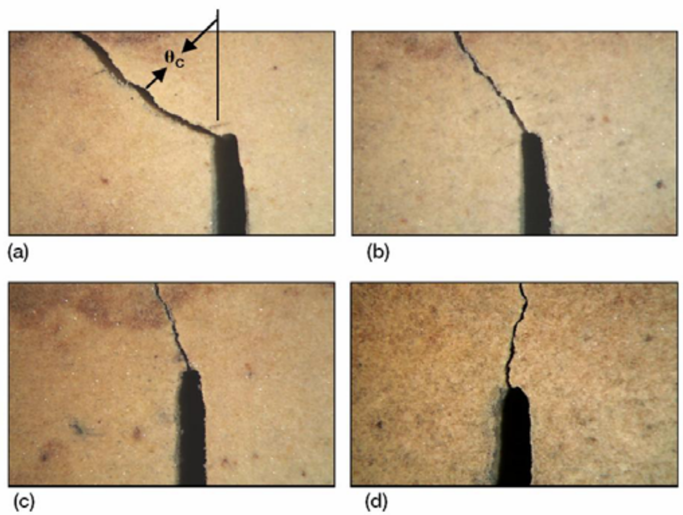

(a) pure mode II, KI/KII = 0; (b) KI/KII = 2.7,

(c) KI/KII = 5.5, and (d) pure mode I, KI/KII =∞

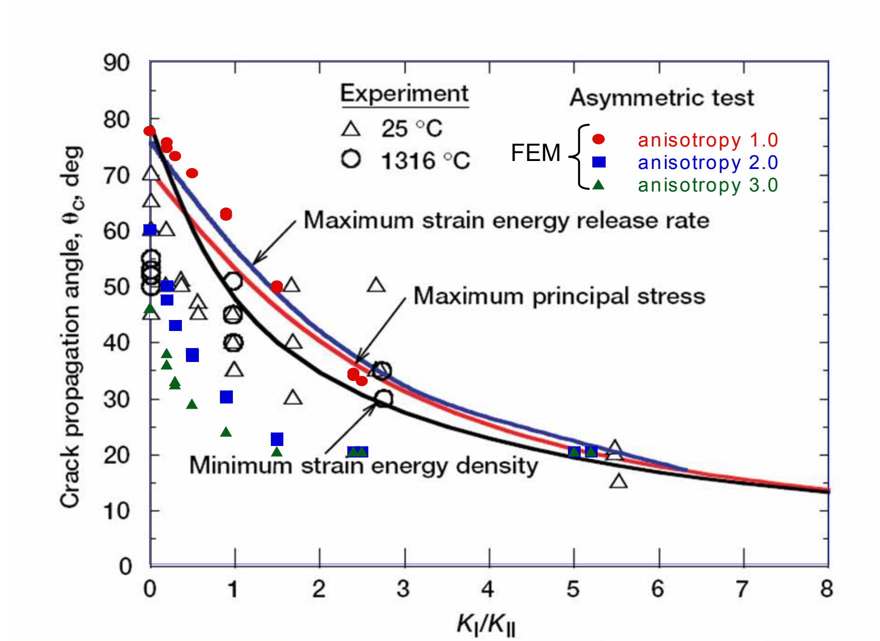

Effect of Material Directionality on Fracture Toughness (K_{IC})

Direction of crack	Fracture Toughness K_{IC} (MPa√m)	Method
Parallel to plasma spray direction	1.15±0.07 (4 specimens)	SEVNB (regular method)
Normal to plasma spray direction	1.04±0.05 (3 specimens)	Double Cantilever Beam (DCB)

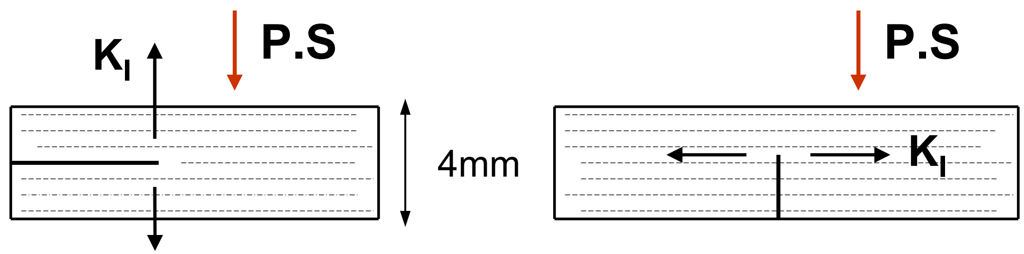

DCB specimen

SEVNB specimen

'P.S': plasma spray direction

Result→ *No significant difference* in K_{IC}-- *No directionality effect* on K_{IC}

Conclusions

- **Mixed mode fracture behavior of TBCs at both 25 and 1316°C follows the *'empirical'* fracture criterion due to the spat microstructure and anisotropic effect as demonstrated by FEM modeling:**

$$\left(\frac{K_I}{K_{IC}}\right)^1 + \left(\frac{K_{II}}{0.65K_{IC}}\right)^2 = 1 \text{ and } \frac{K_{IIC}}{K_{IC}} = 0.65 : \text{ For } 25^{o}\text{C}$$

$$\left(\frac{K_I}{K_{IC}}\right)^1 + \left(\frac{K_{II}}{0.65K_{IC}}\right)^{1.3} = 1 \text{ and } \frac{K_{IIC}}{K_{IC}} = 0.65 : \text{ For } 1316^{o}C$$

- **Prediction of crack propagation angle is also in better agreement when using FEM anisotropic models.**
- **Anisotropy and heterogeneity contributed to the deviation of mixed mode behavior of TBCs**
- **Effect of material directionality on fracture toughness (K_{IC}) was *negligible* (through SEVNB and DCB methods).**